Stress Analysis of External Molten Salt Receiver

Ralf Uhlig[1, a)], Cathy Frantz[2], Robert Flesch[3], Andreas Fritsch[2]

[1a]*Team manager, German Aerospace Center, Institute of Solar Research, Pfaffenwaldring 38-40, 70567 Stuttgart, Ralf.Uhlig@DLR.de*
[2]*Researcher, German Aerospace Center, Institute of Solar Research, Pfaffenwaldring 38-40, 70567 Stuttgart*
[3]*Dr.-Ing.–Researcher, German Aerospace Center, Institute of Solar Research, Prof. Rehm-Strasse 1, 52428 Juelich*

Abstract. Commercial solar thermal power plant projects using central receivers with molten salt as a heat transfer fluid are dominating the market. Due to the complex load situation, especially the inhomogeneous heat flux distribution, the receiver components are subjected to complex thermo-mechanical loads. Transients from operation like clouds, start up and and shut down lead to fatigue of the components. Furthermore, the filling process could be critical due thermal gradients between salt and the metallic components. In this paper, a work flow is presented and results applied at the receiver of the Solar Two experiment to demonstrate the methodology. Thermal models (FE and CFD) are used to deduce the thermal field for different operational situations and a stress analysis is carried out. It was found that highest stresses occur at the absorber tubes for maximum flux density operation (inlet panel). The stresses caused by the filling process are much lower.

INTRODUCTION

The majority of recent commercial solar thermal power plant projects use central receivers with molten salt as a heat transfer fluid. The receiver components, especially the absorber tubes and the headers, are subjected to complex thermo-mechanical loads. Especially the inhomogeneous heat flux distribution leads to stresses caused by thermal gradients. Furthermore, the filling process could be critical due thermal gradients between salt and the metallic components. As commercial projects underlay strict confidential restrictions this paper presents the work flow and results applied at the receiver of the Solar Two experiment to demonstrate the methodology.

In 1992, Simth [1] published a procedure to design and optimize a molten salt receiver. In a first step he reduced the complexity of the load spectrum by grouping the insolation cycles by range, instead of grouping them by range and mean value. (as originally described by Kistler [2]) Furthermore he deduced the allowable flux density on the absorber tubes for a given set of fatigue limits, using the linear damaging rule and correlations for the strain over the circumference of the tubes. [3] In 2016, Sanchez-Gonzalez et al. [4] deduced the allowable flux density caused by thermal stress limits for a molten salt receiver. They based their procedure on the work performed by Irfan and Chapman. [5] They computed the stress caused by the radial thermal gradient in an absorber tube using correlations. [3] In 2016, Doupis [6] performed a fatigue life assessment using a finite element model. A dynamic model of the receiver system was used to determine the temporal and spatial temperature and pressure distribution on the receiver panel during different operation modes (filling, draining, normal operation). In addition the structural FEM model considered structural boundary constraints imposed by the support structure of the panel. The key observations were that transients due to filling and fast temperature changes are the main contributors to the consumption of life of the receiver panel. The draining process had no considerable impact on the lifetime of the component if the MSCR (Molten Salt Central Receiver) is allowed to cool before draining.

In 2016, Du et al. [7] analyzed the thermal stress and fatigue fracture of a tube of a molten salt receiver. A minimum heat flux formula was deduced based on local occurring temperatures and the yield criterion.

METHODOLOGY

As the first step the thermal field of the receiver is calculated with an FE- model generated by the DLR code ASTRID©. The thermal model considers the absorber tubes and the insulations. All relevant boundary conditions like, heat transfer to molten salt, radiation exchange and convection losses to ambient are considered. The solar absorbed heat flux is modeled locally by raytracing [8].

A second FEM model, representing one panel of the receiver, is used for the stress analysis. The model is set up as a thermal- mechanical model. The thermal field of the panel is calculated by mapping the thermal field of the absorber tubes of the ASTRID© receiver model on the mesh of the panel. The headers and connecting tubes are loaded with a heat transfer coefficient and the representative fluid temperature to simulate the header temperature of the observed panel. (Ideal mixing of the absorber flow is assumed, no influence from ovens and insulation).

The mechanical model uses the thermal field for thermal strain calculation. Together with other mechanical boundaries (gravity, pressure, wind forces and supports) displacements and stresses can be calculated for every panel of the receiver. In order to save computation time, the model is subdivided in several sub models in order to analyze the stresses of the parts with the highest occurring stresses.

Thanks to an automated work flow, the thermal field of the panel can be applied for every panel of the receiver without further interference of the user. This allows analyzing the stress situation of the complete receiver in one step for one load case. Fig. 1 shows the principle work flow.

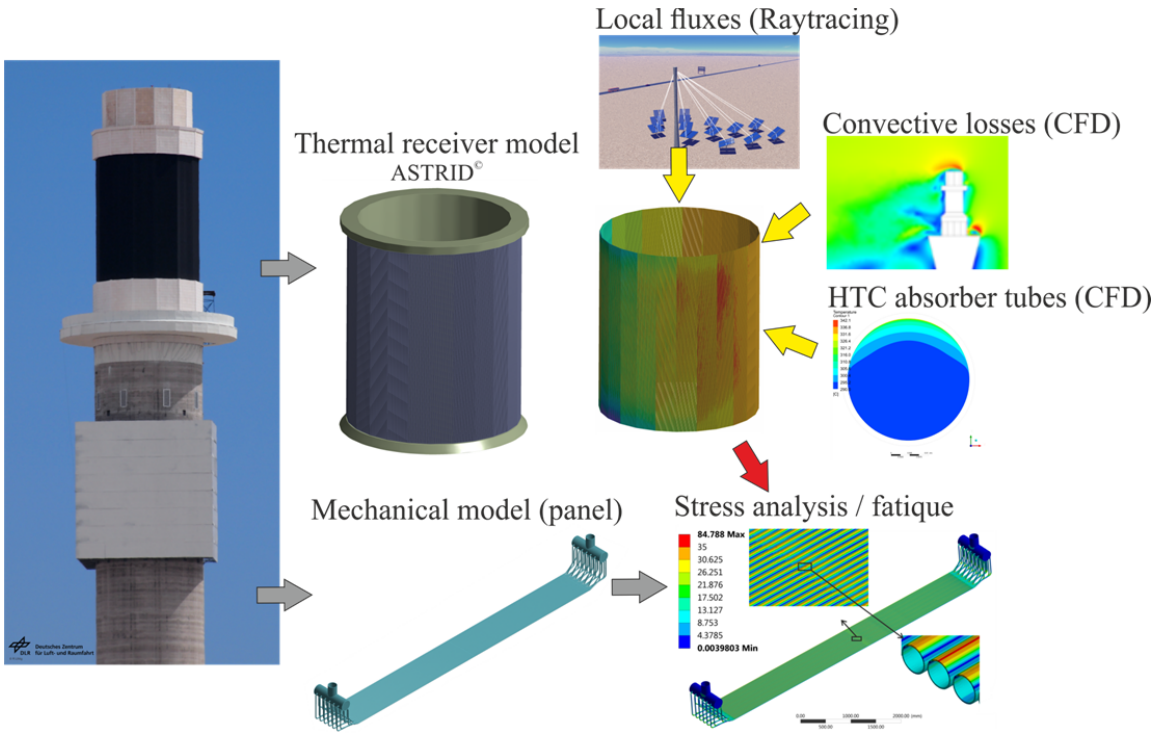

FIGURE 1. Work flow stress analysis

The same FE model of the panel is used to analyze the stresses during the filling process. In comparison to the simulation of the solar operation, the thermal field is calculated with a transient thermal model. For this purpose, a transient, two-phase (air and molten salt) CFD analysis is performed in order to deduce the local and temporal heat transfer coefficients during the filling process. The resulting heat transfer coefficients are then applied in the FE model as a forced convection boundary condition at the inside of the absorber tubes, connection pipes and the header tube. In addition, the solar heat flux of the pre-heating process, as well as convection and radiation to ambient are considered. Finally the headers are heated to a specific temperature by using a forced convection boundary condition. This represent temperature controlled heating of headers by radiators.

SIMULATION OF THERMAL FIELD OF RECEIVER PANEL

The thermal field of the receiver was analyzed using a three-dimensional thermal FE- model of the absorber tubes and the insulation. The presented results are performed for the receiver of the Solar Two experiment, which was operated during the late 90's by the Department of Energy in Daggett, California. The receiver of the Solar Two experiment consisted in 24 absorbing panels, each composed of 32 parallel tubes (inner diameter 18.6 mm; wall thickness 1.2 mm; length 6.2 m), mounted in a vertical fashion. The panels were arranged in a polyhedron shape, thereby approximating a cylinder [9].

Within this model the absorber tubes are considered with a moderate mesh resolution (16 elements over circumference, 50 over length). This allows a 3D simulation of the complete receiver with acceptable computational effort. Beside the overall thermal results, such as efficiency, thermal power, heat losses and fluid temperatures, the model provides also the local 3-dimensional temperature distribution of the absorber tubes.

The solar radiation reflected by the heliostat field on the receiver aperture is not only dependent on the sun's azimuth and elevation angle, but is also influenced by other optical circumstances such as mirror reflectivity, tracking errors etc. The heat flux absorption capability of a molten salt receiver panel is limited. Also in the case of the Solar Two heliostat field, the maximum deliverable heat flux exceeds this limit. For this reason a parametric aiming point assignment method is used to deduce individual aiming points for the heliostat field. [10] This leads to an inhomogeneous and complex heat flux distribution on the receiver. Based on the published data of the Solar Two heliostat field [9], a representative heat flux distribution on the receiver aperture was computed using a ray tracing code. The geometry of absorber tubes is directly represented by the FE- mesh in this raytracer code.

The heat transfer to the fluid is modeled using one-dimensional fluid flow elements allowing mass and thermal transportation. The heat transfer coefficients are calculated as a function of the mass flow in the tube, using the Gnielinski Nusselt correlation [11]. For the computation of the fluid properties the temperature-dependent correlations published in [9] are used. The thermal radiative exchange between the absorber tubes and the insulation as well as the radiation to the ambient is considered by the radiosity method. The convection to ambient is considered on half of the tube surface (ambient side) using a heat transfer coefficient and the ambient temperature.

The model was validated by re- calculating three measurement points of the Solar Two experiments in [12] resulting in a very good agreement between measurements and simulations.

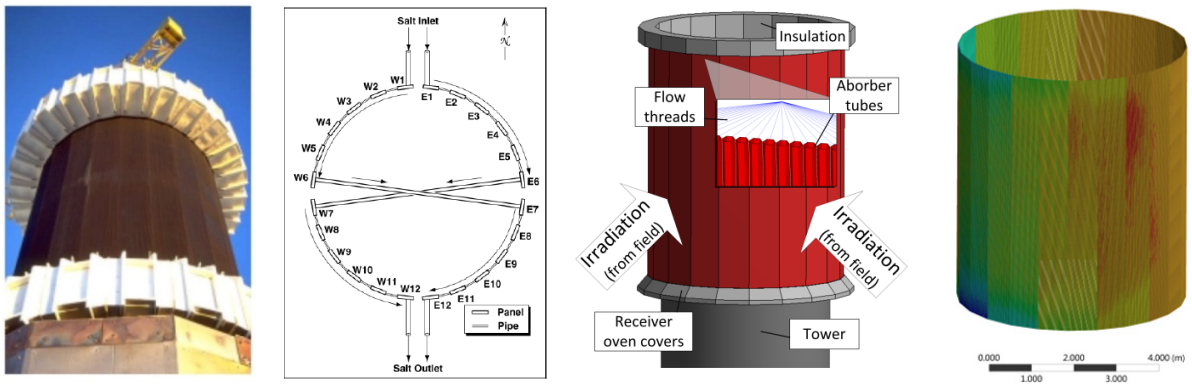

(a) (b) (c) (d)

FIGURE 2. (a) (b) Receiver Solar Two experiment [9], (c) ASTRID© receiver model, (d) Thermal field receiver

MODELLING THE FILLING PROCESS WITH CFD

For a detailed analysis of the heat transfer from wall to the fluid during the filling procedure, a multiphase transient CFD model was used. The filling was simulated for one single tube and at the geometry of the collector and the connecting pipes. All CFD simulations were carried out with ANSYS CFX. Turbulence was modeled with the k-ω-SST turbulence model. A homogeneous approach for the two phase flow was chosen, in which the same velocity of salt and air in a cell is assumed. A limit of $1 \cdot 10^{-4}$ was used for the residuals and the Courant number was kept below 2.

Absorber Tube

As the tubes of a molten salt receiver are filled parallel the filling process is similar in all absorber tubes and therefore this simplification can easily be justified. To reduce the computational effort furthermore, only half of the tube is simulated and a symmetry plane in the center of the tube is assumed. The backside of the tube is assumed to be adiabatic.

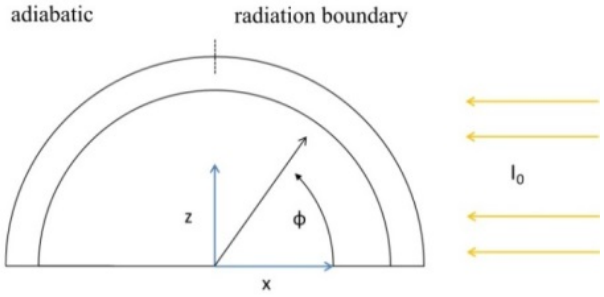

$$\dot{q} = I_0 \, \epsilon \, \frac{x}{\sqrt{x^2+z^2}} - \epsilon\sigma(T^4 - T_U^4) - \alpha(T - T_U) \quad (1)$$

FIGURE 3. Cross section of the simulated domain in the CFD model

On the front part the following boundary condition is used combining the heat flux density $\dot{q}$ with the local temperature T for a given ambient temperature T_U, a convective heat transfer coefficient α and an emissivity/absorptivity of the tube ϵ.

The mesh was refined until in a steady state simulation for a filled tube and a mesh with 272 fluid elements in the cross section and 500 elements in lengthwise direction an almost mesh independent temperature was reached. In this mesh the dimensionless wall distance is approximately 1.5. For the tube a resolution of 51 elements in the cross section was found sufficient for an accurate solution.

The simulations used in the following were carried out for an incoming flux density of $I_0 = 20\ \mathrm{kW/m^2}$, a convective heat transfer coefficient $\alpha = 7.7\ \mathrm{W/(m^2K)}$ with an ambient temperature of 20°C and a mass flow of $0.074\ \mathrm{kg/s}$. The transient filling simulation is started from the steady-state solution of the tube with an air flow with the velocity corresponding to the salt velocity at a mass flow of $0.074\ \mathrm{kg/s}$. For the stress analysis of the tube the heat transfer coefficient from the inner tube wall to the salt/air is of special interest. The Nusselt number is shown in Fig. 4 (a) for different times. Due to entrance effect at the inlet of the tube the heat transfer coefficient is extremely high close to the inlet. Additionally, as it has already been reported in Flesch et al. [13], a second region with increased heat transfer can be observed close to the interface of salt and air. During the filling process, the described region moves upwards, together with the air-salt interface. The effects causing the increased heat transfer are similar to those at the inlet of the tube: The interface between salt and air moves with a homogeneous velocity. The salt close to the wall just beneath the interface is slowed down as a result of the influence of the wall. Therefore, the salt filling the parts at the wall originates from the more central and thereby colder parts of the fluid cylinder. Hence, cold salt gets in contact with the hot wall resulting in a very high heat transfer.

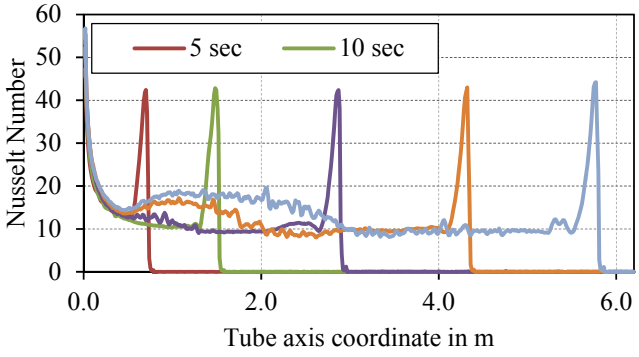

FIGURE 4. Heat transfer coefficient as function of position in tube for different times

With increasing vertical distance from the interface the heat transfer decreases as the thermal boundary layer converges into a developed state. The resulting local and temporal heat transfer coefficients were used for the detailed thermal simulation of the wall to evaluate the stresses caused by non-uniform cooling.

Header

Using the same approach as for the absorber tubes, the filling of the collector was simulated using CFD. In this case a tetrahedron mesh with prism layers was used. Mesh independence study resulted in a mesh size of about four million elements. As the collector is located within an insulated region (oven) and is heated by radiators a constant heat transfer coefficient of 10'000 W/m^{2}K with an ambient temperature of 400°C was modelled at the outer surfaces of the header and connecting tubes. (This boundary condition is chosen to represent a temperature controlled heating of the header). Fig. 5 (a) shows the volume fraction between air (blue) and salt (red) after a simulation time of 50s. It can be seen that the geometric arrangement of the connecting tubes leads to a very inhomogeneous flow distribution. The horizontal parts of the tubes are not filled completely. This situation exists until the fluid level within the collector tube raises up to the holes of connection tubes and then this connection tube starts to be filled completely. Following heat transfer to the fluid is inhomogeneous as shown in Fig.5 (b).

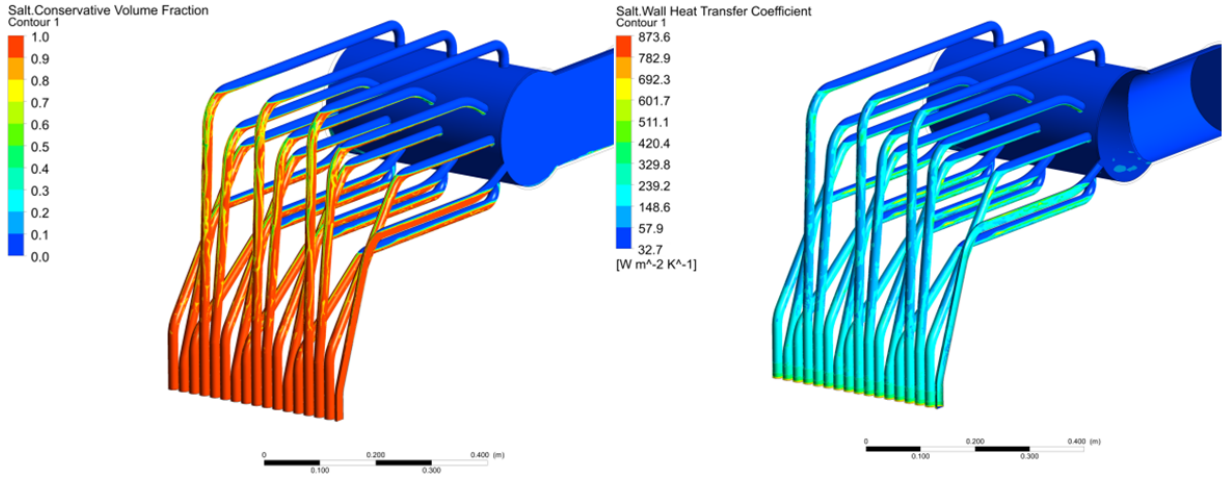

FIGURE 5. CFD model filling header (a) Volume fraction of air (blue) and salt (red) after 50s filling time, (b) Heat transfer coefficients (based on fluid bulk temperature of 350°C)

STRESS ANALYSIS

The results of the thermal simulations were used to calculate the thermal strain using the mechanical FE- model of the panel. Together with other mechanical loads, such as pressure (pressure of 10Bar all inside faces) and supports (end face of inlet header is in circumferential and longitudinal direction fixed, outlet header is parallel to inlet header), stresses were calculated for different load situations. The local stresses of the components are analyzed in detail using sub models of the component with the highest loads. For this purpose the displacement at the boundaries as well as the local temperatures are taken from the complete mechanical model.

Solar Operation

The thermo-mechanical FE model of the panel uses the appropriate thermal field of the panel from the receiver simulation by mapping the temperature distribution of the absorber tubes to the equivalent tubes of the panel. The headers and connection tubes, which are not considered within the receiver model, are loaded with a forced convection boundary using an averaged heat transfer coefficient and fluid temperature. (Ideal mixing of the absorber flow is assumed). Subsequently stresses were evaluated, first for the complete model, secondly for the part with the highest stresses using a sub model.

Filling

To analyze the stresses during the receiver filling process the thermo-mechanical FE model of the panel is solved by using the local transient heat transfer coefficients and fluid temperatures from the CFD filling model as a forced convection boundary condition on the inner surfaces of the components. At the outside faces of the absorber tubes (ambient side) the pre- heating by solar radiation is represented using a sinusoidal distributed heat flux with a peak value of $20\ \mathrm{kW/m^2}$. Radiative exchange between the tubes and the ambient was modelled using the radiosity method. Convection to ambient was modelled with a forced convection boundary with a heat transfer coefficient of $7\mathrm{W/m^2K}$ and an ambient temperature of 20°C. The outer surfaces of the header and connection tubes are loaded with a forced convection boundary condition representing the heat input from the oven.

In opposite to the solar operation simulations, the thermal field is calculated in a transient fashion to resolve time depending thermal gradients. Subsequently stresses are evaluated, first for the complete model, secondly for the part with the highest stresses using a sub model. The stresses are analyzed for different time points of the transient thermal simulation.

RESULTS

Solar Operation

The results show that stresses within the absorber tubes are highest at solar operation at design point. In this case the thermal gradients over the circumference of the absorber tube are highest (Fig. 6). (Max. values in the plot are located at singularities within the model and are not evaluated). Especially the panels with the highest solar load (inlet panels) show the highest gradients and stresses (Fig. 7).

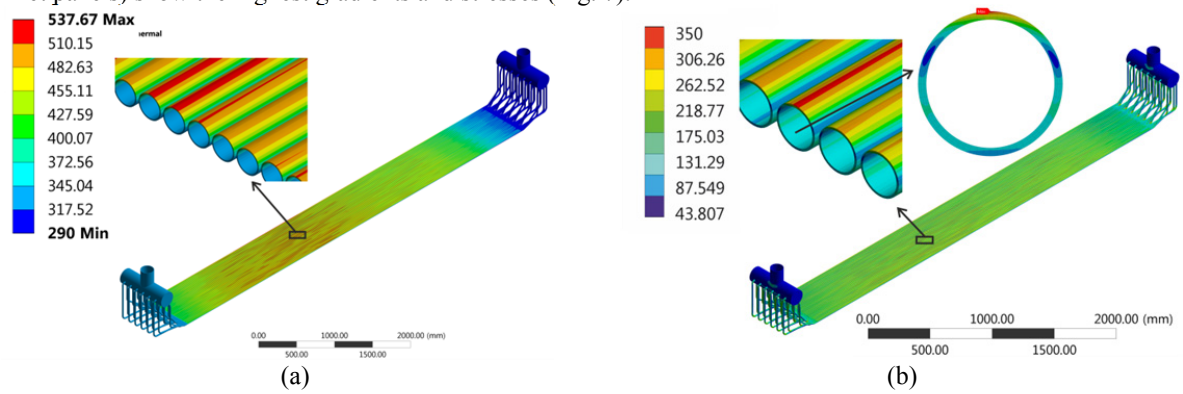

(a) (b)

FIGURE 6. Results solar operation (a) thermal field panel W1 [°C], (b) Equivalent stresses (Mises) [MPa]

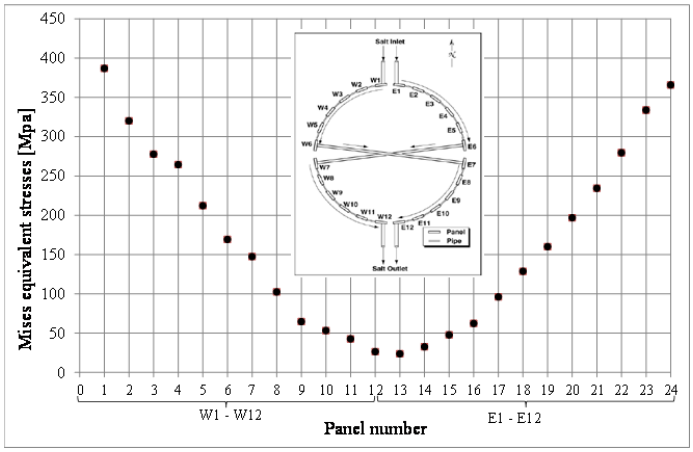

FIGURE 7. Equivalent stresses (Mises) [MPa] of the different panels

Filling

The results of the stress analysis of the filling process show that the stresses at the absorber tubes are mainly caused by the thermal gradient from the one-side heating of the panel. Fig. 8 shows the thermal field and the stresses of the panel after a filling time of 20s. In comparison to the stresses during solar operation, the stresses are about 10 time lower.

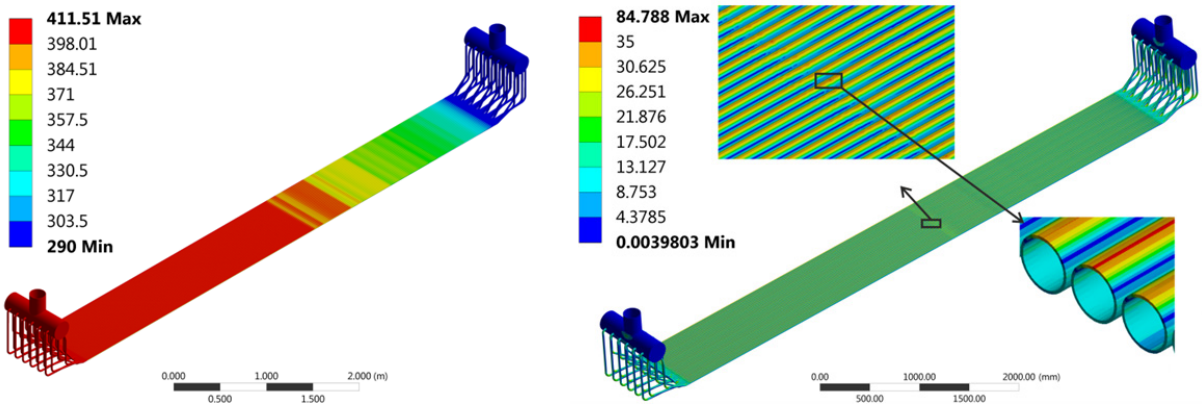

(a) (b)

FIGURE 8. Results panel filling (a) thermal field header after 20s [°C], (b) Equivalent stresses (Mises) [MPa]

Due to the higher thermal mass of the collector tube, the filling procedure causes stresses when the connecting pipes are cooled down by the fluid. Highest stresses were found after a time of 80s (Fig. 9).

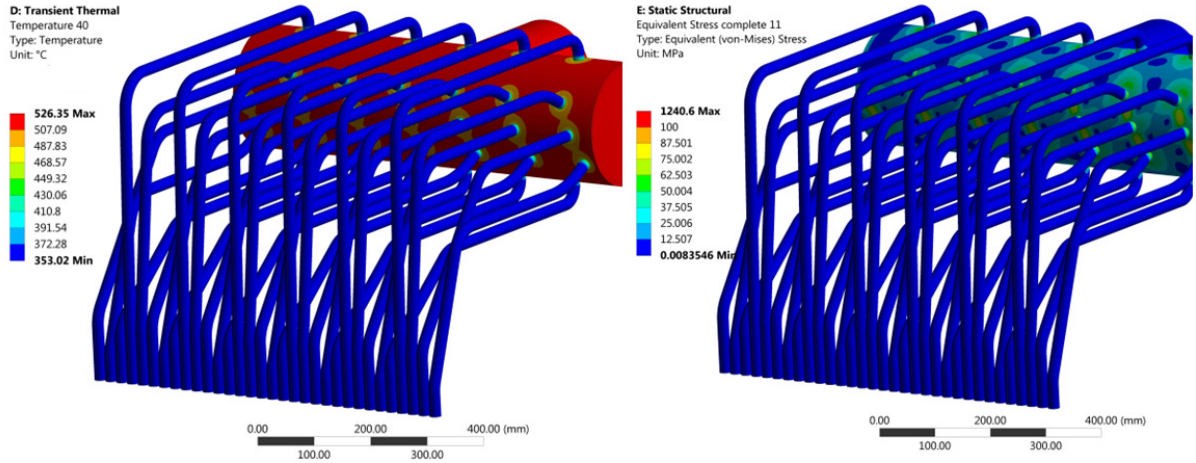

(a) (b)

FIGURE 9. Results filling (hot header) (a) thermal field header after 80s [°C], (b) Equivalent stresses (Mises) [MPa]

CONCLUSIONS AND OUTLOOK

Nowadays, advanced simulation tools allow detailed analyzing of complex loaded external molten salt receivers. A 3D thermal receiver model with all relevant thermal boundaries allows the simulation of the temperature distribution over the receiver. Especially the consideration of the local solar flux distribution and the local fluid temperature are leading to a realistic temperature field over the absorber tubes.

This thermal data was used to calculate the stresses within the panels of the Solar Two receiver with a 3D thermo- mechanical model of one panel. The local stresses are analyzed in detail using sub modelling. This approach

allows economic simulation efforts as the mesh density is adapted to the field of interest. Furthermore the automated approach allows the stress calculation of the complete receiver for one load case in one run. Consequently other load cases (part load, special operation) can be calculated with the same approach. The outcome of this is a load collective of the receiver components which can be further used for fatigue analysis using standard design codes (ASME Boiler Vessel Code for example). The presented methodology can be used at the design phase of receiver to optimize the design and estimate the life time of components. During the operation phase this approach can be used to monitor the life time of the components according to the "real" load situation. Therefore the thermal receiver simulation has to be set up with the solar flux distribution, mass flow of the salt, wind speed and direction and the ambient temperature according to the operation data.

For the future it is planned to include this approach in an overall control system. As the computational effort will not allow real-time simulation, the idea is to pre- run several load cases. The results can be stored in a data base, allowing the control system to estimate the best operation strategy in order to maximize life time.

In comparison to the stresses from solar operation, the stresses from the filling process are much lower.

ACKNOWLEDGMENTS

This work was partly supported by the Federal Ministry for Economic Affairs and Energy (BMWi) based on a decision of the German Bundestag. Funding codes: 0325733A, 0325655, 0325756.

REFERENCES

1. Simth, D. C., *Design and optimization of tube-type receiver panels for molten salt application* (Solar Engineering Vol. 2, 1029 – 1036, 1992)
2. Kistler, B., *Fatigue Analysis of a Solar Central Receiver Design Using Measured Weather Data* (Sandia National Laboratories, Albuquerque, New Mexico (USA),1986).
3. Young, W., & Budynas, R. (2002). Roark's Formulas for Stress and Strain. New York: McGraw-Hill.
4. Sánchez-González, A., Rodríguez-Sánchez, M., & Santana, D., *Aiming strategy model based on allowable flux densities for molten salt central receivers* (Solar Engery, 2016).
5. Irfan, M., & Chapman, W., *Thermal stresses in radiant tubes due to axial, circumferential and radial* (Applied Thermal Engineering 29, S. 1913–1920, 2009).
6. Doupis, D., & Wang, C., *Transient Simulation of Molten Salt Central Receiver* (AIP Conference Proceedings 1734, 2016)
7. Du, B.-C., He, Y.-L., Zheng, Z.-J., & Cheng, Z.-D., *Analysis of thermal stress and fatigue fracture for the solar tower* (Applied Thermal Engineering 99, S. 741-750, 2016)
8. C. Frantz, A. Fritsch, and R. Uhlig, *ASTRID© – Advanced Solar Tubular ReceIver Design: A powerful tool for receiver design and optimization* (AIP Conference Proceedings 1850, 030017, 2017)
9. Pacheco, James E., *Final Test and Evaluation Results from the Solar Two Project* (Albuquerque, New Mexico : Sandia National Laboratories, 2002).
10. R. Flesch, C. Frantz, D. Maldonado, P. Schwarzbözl, *Towards an optimal aiming for molten salt power towers* (Solar Energy 155 (1273-1281), 2017)
11. Verein Deutscher Ingenieure, *VDI-Wärmeatlas* (10. Aufl. Springer-Verlag, Berlin, 2006)
12. Uhlig, Ralf und Frantz, Cathy und Fritsch, Andreas, *Effects of vertically ribbed surface roughness on the forced convective heat losses in central receiver systems* (Proceedings SolarPACES 2015 Conference, 1734. AIP Conference Proceedings, 13.-16. Okt. Cape Town, South Africa, 2015)
13. R. Flesch, D. Högemann, J. Hackmann, R. Uhlig, P. Schwarzbözl, G. Augsburger, and M. Clark, *Dynamic Modeling of Molten Salt Power Towers* (SOLARPACES 2016: International Conference on Concentrating Solar Power and Chemical Energy Systems, AIP Conference Proceedings 1850, edited by A. Obaidli et al. (American Institute of Physics, Melville, NY, 2017)